Reduction of *all-trans*-Retinal in the Mouse Liver Peroxisome Fraction by the Short-Chain Dehydrogenase/Reductase RRD: Induction by the PPARα Ligand Clofibrate†

Zhen Lei, Weiguo Chen, Min Zhang, and Joseph L. Napoli*

Department of Nutritional Sciences and Toxicology, 119 Morgan Hall, MC#3104, The University of California, Berkeley, California 94720

Received October 3, 2002; Revised Manuscript Received January 10, 2003

ABSTRACT: The mouse liver 16000*g* fraction, which contains peroxisomes, reduces *all-trans*-retinal, but has limited ability to dehydrogenate retinol enzymatically. Feeding mice for 2 weeks with a diet containing clofibrate (0.5%, w/w), a PPARα ligand and peroxisome proliferator, increased the 16000*g* fraction ∼2-fold in protein, ∼2-fold in specific activity of retinal reduction, and ∼4-fold in retinal reductase units compared to controls, and caused a 50% decrease in liver retinol. An increase in both reductase specific activity and units indicates that clofibrate/PPARα induced expression of retinal-reducing enzymes(s), in addition to increasing reductase(s) content. We expressed a cDNA from the NCBI data bank that encodes a peroxisome short-chain dehydrogenase/reductase. The enzyme, mouse retinal reductase (RRD, also known as human 2,4-dienoyl-CoA reductase), reduces *all-trans*-retinal [$V_m = 40$ nmol min^{-1} (mg of protein)$^{-1}$; $K_{0.5} = 2.3$ μM] and has 4- and 60-fold less activity with 13-*cis*-retinal and 9-*cis*-retinal, respectively. Recombinant RRD functions with both unbound and CRBP(I) (cellular retinol-binding protein)-bound retinal, but apo-CRBP(I) inhibits the reductase. RRD mRNA expression was initiated on embryo day 7. Most adult tissues assayed expressed the mRNA. Liver, kidney, and heart had the most intense expression, with much less intense expression in brain, spleen, and lung. Clofibrate feeding increased the amount of RRD protein in the 16000*g* fraction of liver, consistent with the clofibrate-induced increase in reductase activity. These data relate retinoid metabolism, PPARα, peroxisomes, and RRD, and are consistent with a further function of CRBP(I) in retinoid metabolism.

Vitamin A (*all-trans*-retinol) supports vision, fertility, and embryogenesis, contributes to regulation of intermediary metabolism, and maintains normal epithelia, bones, nerves, and immunity in all vertebrates (*1*−*6*). Vertebrates fulfill their needs for vitamin A through absorption of preformed dietary retinol and through oxidative central cleavage of carotenoids into *all-trans*-retinal, followed by reduction into *all-trans*-retinol (*7*−*9*). Retinol does not support vitamin A functions directly, but requires conversion into atRA[1] (*10*). atRA binds with the ligand-activated transcription factors, RARα, -*β*, and -*γ*, which belong to the superfamily of nuclear receptors, and thereby controls the expression and function of numerous genes (*11*−*13*).

Interest in enzymes that control retinol homeostasis and conversion into atRA has been heightened because of the emerging insight that appropriate vitamin A function depends on regulation of retinol metabolism (*14*). Although several SDRs have been cloned and characterized in mouse, rat, bovine, and human that catalyze the dehydrogenation of retinol and/or the reduction of retinal, mRDH1 is the only one in the mouse with widespread expression starting early during embryogenesis, and with high dehydrogenation efficiency for *all-trans*-retinol (*15*). In intact cells, mRDH1 functions in the oxidative direction, and constitutes a path of atRA biosynthesis in association with any one of RALDH1, -2, or -3. atRA generation from dehydrogenation of *all-trans*-retinal would represent a controlled process, for minimizing the steady-state concentration of the intermediate *all-trans*-retinal, because of the potential toxicity of retinal and atRA, and the essentiality of the time and locus requirements for atRA (*5*).

Most known enzymes and binding proteins that contribute to retinoid metabolism localize to cytosol (cellular retinol-binding proteins and retinal dehydrogenases) and microsomes (lecithin:retinol acyltransferase, retinol dehydrogenases, retinyl ester hydrolases, and CYP26) (*14*, *16*−*18*). Other cellular components, however, participate in lipid metabolism. Some of the steroid hormone biosynthetic enzymes localize in mitochondria (*19*), and the RA binding protein CRABP(I) may localize to mitochondria (*20*). Peroxisomes also provide a metabolically significant site of lipid biosynthesis and catabolism (*21*). For example, peroxisome enzymes contribute to the conversion of cholesterol into bile acids, are largely responsible for *β*-oxidation of long-chain and branched-chain fatty acids, and contribute to oxidation of excess dietary fatty acids. Yet little effort has been reported concerning retinoid metabolism outside cytosol and microsomes.

† This work was supported by Grant DK47839 from the National Institutes of Health.

* To whom correspondence should be addressed: Department of Nutritional Sciences and Toxicology, 119 Morgan Hall, MC#3104, The University of California, Berkeley, CA 97420-3104. Phone: (510) 642-0908. Fax: (510) 642-0535. E-mail: jna@uclink4.berkeley.edu.

[1] Abbreviations: atRA, *all-trans*-retinoic acid; CRBP, cellular retinol binding protein; PPAR, peroxisome proliferator-activated receptor; RE, retinyl ester(s); RRD, retinal reductase; SDR, short-chain dehydrogenase/reductase.

10.1021/bi026948i CCC: $25.00
Published on Web 03/19/2003

Generation of *all-trans*-retinal by carotenoid cleavage, although a necessary component of normal vitamin A nutriture, presents a potential problem for vertebrates by generating bolus retinal concentrations that could drive atRA biosynthesis into the toxic range (*22*). A mechanism of preventing excess intestinal retinal oxidation seems to be imparted by expression of CRBP(II), a retinoid-specific binding protein that allows retinal reduction but not oxidation (*23*). A second potential mechanism for preventing high and potentially toxic steady-state concentrations of retinal would involve expression of retinal reductase(s) in tissues that cleave carotenoids but do not express CRBP(II). In this report, we characterize a retinal reductase, RRD, in mouse liver peroxisomes that reduces retinal in the absence or presence of CRBP(I) into retinol, and which is inhibited by apo-CRBP(I). We also observed that clofibrate, a PPARα ligand and peroxisome proliferator, induces RRD activity and reduces the level of liver retinol.

EXPERIMENTAL PROCEDURES

Mouse Liver 16K Fraction. Male C57BL6J mice (3−4 months old from Charles River) were fed a stock diet containing clofibrate (0.5%, w/w) for 2 weeks; control mice were fed an identical diet without clofibrate. Mice had free access to food and water. After 2 weeks, mice were fasted overnight and sacrificed by cervical dislocation under CO_2 narcosis. Livers were excised, weighed, and minced on a cold glass plate. Minced liver was suspended in 2.5 mL of ice-cold homogenization buffer [10 mM Hepes (pH 7.5), 250 mM sucrose, 1 mM EDTA, and 2 mM DTT] and homogenized with a Kontes Duall tissue grinder. The light mitochondria fraction, which contains mitochondria, peroxisomes, and lysosomes, was prepared by standard differential centrifugation at 4 °C (*24*−*26*). Briefly, the homogenate was centrifuged at 1000*g* for 10 min. The supernatant was centrifuged at 2800*g* for 15 min. The second supernatant was centrifuged at 16000*g* for 10 min. The 16000*g* pellet was resuspended in homogenization buffer to produce the 16K fraction. Catalase activity in the 16K fraction was assayed spectrophotometrically at 240 nm as described (*27*). Protein concentrations were measured by the Bradford method (*28*).

Quantification of Liver Retinoids. A 25% homogenate in water (w/v) was prepared from each mouse liver, and aliquots of each (5% of the totals) were extracted as described, up to and including the precolumn procedure using an anion-exchange resin (*29*). Aliquots of each extract (5%) were quantified by high-performance liquid chromatography using a Waters Resolve C-18 column eluted at 1 mL/min with A (15% water/85% methanol) for 13 min and then a linear gradient of A to B (30% dichloroethane/70% methanol) developed from 13 to 17 min, continuing with B from 17 to 30 min. Retinol eluted at 11 mL, and retinyl palmitate eluted at 27 mL. Peak areas (325 nm) were compared to areas of retinol and retinyl palmitate peaks generated from authentic standards.

Enzyme Assays with Retinoids. Assays were carried out in 0.25 mL of 50 mM Hepes (pH 8), 150 mM KCI, 1 mM EDTA, 2 mM DTT, and 2 mM pyridine nucleotide cofactor. NADPH was generated in a 5 min preincubation with glucose-6-phosphate dehydrogenase (2.5 units), $NADP^+$ (500 nmol), and glucose 6-phosphate (0.5 μmol). Kinetic constants for recombinant RRD were determined under initial velocity conditions: the reaction was linear to 7.5 min and 10 μg of protein. Reactions were quenched with 0.3 mL of 0.1 M *O*-ethylhydroxylamine in 0.1 M Hepes and 0.5 mL of methanol, followed by incubation for 30 min at room temperature to produce retinal oximes. Retinol and retinal oximes were extracted with hexane (3 mL). The hexane phases were evaporated with nitrogen, and the residues were dissolved in 0.1 mL of hexane and applied to high-performance liquid chromatography to quantify retinoids as described (*15*, *30*).

cDNA Cloning. Reverse transcription of mouse liver mRNA (Sigma) was carried out with the M-MLV reverse transcriptase system (Invitrogen). The cDNA of the RRD coding region was amplified with the sense primer 5′-TCCCCTAGCAGAGTTCAAC and the antisense primer 5′-GTTAGGTGGTGGCAACGA. Amplification was carried out for 2 min at 94 °C and for 35 cycles of 1 min at 94 °C, 1 min at 55 °C, and 1.5 min at 72 °C, followed by a final incubation at 72 °C for 5 min. This PCR product was used as a template with the sense primer 5′-CCGGAATTC**GCCGCCACC**ATGCAGAAAGCG (the *Eco*RI site underlined and the Kozak sequence in bold and underlined) and the antisense primer 5′-CCGCTCGAGTCAGAGGCGAGAAGG (the *Xho*L site underlined). The PCR product was gel-purified, digested with *Eco*RI and *Xho*I, and cloned into the *Eco*RI and *Xho*I sites of pcDNA3 (Invitrogen) to construct pcDNA3/RRD.

Recombinant RRD Expression. CHO-K1 cells (ATCC) were cultured at 37 °C in Ham's F12 medium supplemented with 10% fetal calf serum. Cells were transfected with pcDNA3/RRD or pcDNA3 (8 μg/100 mm plate) using Lipofectamine (Gibco), harvested 24 h later, and lysed by sonication in 20 mM Hepes, 150 mM KCl, 1 mM EDTA, 10% sucrose, and 2 mM DTT (pH 7.5). The supernatants obtained by centrifuging lysates at 800*g* for 10 min were used for enzyme assays.

Intact Cell Assays. CHO-K1 cells cultured in six-well plates were transfected with pcDNA3, pcDNA3/RRD, or pcDNA3/RDH1 (each at 2 ng/well) (*15*). Twenty-four hours later, the medium was replaced with fresh medium. Transfected cells were incubated with 2 μM *all-trans*-retinal or *all-trans*-retinol for 30 min. The reactions were quenched with methanol and *O*-ethylhydroxylamine, and retinoids were extracted and assayed as described above.

Northern Blots. Northern blot analysis was carried out with the commercial mouse multiple-tissue Northern blot (Clontech), which contains 2 μg of poly(A^+) RNA per lane on a Nylon membrane. A 3′-UTR cDNA probe, corresponding to nucleotides 876−1200 of RRD, was labeled with ^{32}P using the the RadPrime DNA Labeling system (Promega). The probe was purified with a Micro Bio-Spin 30 Column (Bio-Rad), and was hybridized with ExpressHyb hybridization solution at 60 °C for 1 h according to the manufacturer's protocol. The blot was washed three times in 2× SSC with 0.05% SDS at room temperature for 30 min, followed by two washes in 0.1× SSC with 0.1% SDS for 40 min at 50 °C. The membrane was exposed to X-ray film with an intensifying screen for 3 h at −70 °C.

RNA Blots. The RRD probe used for Northern blots was hybridized to a mouse RNA Master Blot according to the

Table 1: Effect of Clofibrate on *all-trans*-Retinal Reduction in the 16K Fraction of Mouse Liver[a]

expt	*n*	group	protein (mg)	specific activity [nmol min^{-1} (mg of protein)$^{-1}$]	units [nmol min^{-1} (16K fraction)$^{-1}$]
1	3	control	9.3 ± 0.6	0.5 ± 0.1	4 ± 0.5
	3	dosed	17.1 ± 2.8	0.8 ± 0.1	13 ± 2
2	5	control	9.3 ± 0.2	0.5 ± 0.1	4.2 ± 0.7
	5	dosed	17.4 ± 2.3	1.0 ± 0.1	19.1 ± 4

[a] Clofibrate or vehicle alone was administered to mice for 14 days. *all-trans*-Retinal reactions were carried out with 5 μM substrate for 5 min with 50 μg of protein and 2 mM NADPH. Amounts of protein, specific activities, and units in the control vs the treated groups differ significantly from each other ($p < 0.025$). Assay of the peroxisomal enzyme catalase in the 16K fractions of experiment 2 from control and clofibrate-treated liver showed specific activities of 0.22 ± 0.04 and 0.35 ± 0.04 mmol min^{-1} (mg of protein)$^{-1}$, respectively, and contents of 2.1 ± 0.2 and 6.6 ± 2.8 mmol/min, respectively. All data are the means ± standard deviation (*n* is the number of mice per group). The 16K fractions from each mouse liver were assayed individually in triplicate.

Table 2: Amino Acid Comparisons of SDR that Catalyze Retinoid Metabolism

species	enzyme	% identity	% similarity	GeneBank entry
mouse	RRD	100	100	AB045132
human	RRD	80.3	86.4	AB045131 and AF044127
human	retSDR1	21.1	31.4	AF061741
mouse	CRAD1	17.0	29.3	AF030513
mouse	CRAD3	16.9	29.8	AF372838
human	PR-RDH	16.7	28.2	AF229845
mouse	RDH1	16.7	29.9	AY028928
human	RalR1	16.5	28.9	AF167438

manufacturer's protocol (Clontech). Briefly, the membrane was prehybridized for 30 min at 65 °C in 10 mL of ExpressHyb solution. Hybridization was carried out at 65 °C overnight with a cDNA probe mix that included 30 pg of Cot-1 DNA and 150 μg of sheared salmon testes DNA. The blot was washed five times in 2× SSC with 1% SDS at 65 °C for 20 min, followed by two 20 min washes in 0.1× SSC with 0.5% SDS at 55 °C for 20 min. The dot blot was exposed to X-ray film at −70 °C for 48 h with an intensifying screen.

Western Blots. Rabbit anti-peptide antibodies were raised from the RRD peptide SVLWEEKAREDFIKE conjugated with KLH and were affinity purified. This peptide was selected because it is not similar to any of the SDRs listed in Table 2, or any other known SDR. Equivalent amounts of the mouse liver 16K protein were separated by 15% SDS−PAGE and blotted onto nitrocellulose membranes. Membranes were incubated with 5% nonfat milk in 0.2% PBS-T overnight at room temperature, and were then incubated with anti-RRD antipeptide antibody (1:2000, v/v) in 0.2% PBS-T with 1% nonfat dry milk for 1 h at room temperature, followed by five washes in 0.2% PBS-T for 10 min each. Membranes were incubated with alkaline phosphatase-conjugated anti-rabbit IgG for 1 h at room temperature, and were washed as described above, followed by an additional wash with 100 mM Tris-HCl (pH 9.5), 100 mM NaCl, and 5 mM $MgCl_2$. Protein bands were visualized using a commercially available NBT/BCIP color development substrate (Promega).

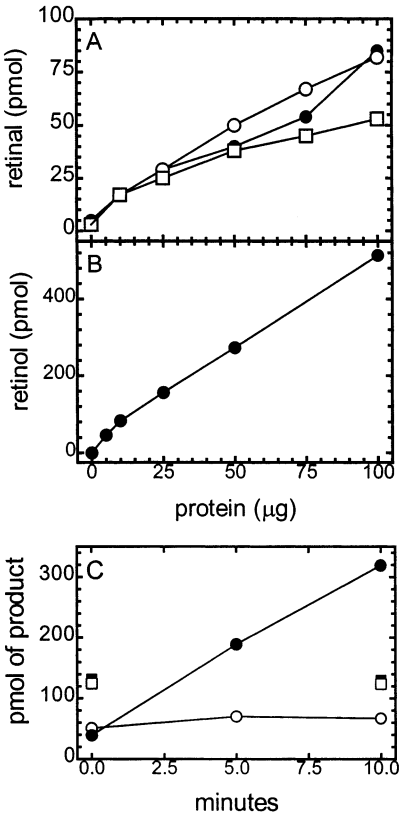

FIGURE 1: Retinoid dehydrogenation vs reduction in the mouse liver 16K fraction. (A) Oxidation of *all-trans*-retinol was assessed at 4 °C for 0 min (□), 25 °C for 5 min (○), or 37 °C for 5 min (●) in the presence of 2 mM $NADP^+$. (B) Reduction of *all-trans*-retinal was assessed at 37 °C for 5 min in the presence of 2 mM NADPH. (C) Oxidation of *all-trans*-retinol was assessed at 37 (■) or 25 °C (□). Reduction of *all-trans*-retinal was assessed at 37 (●) or 25 °C (○). Each reaction used 5 μM substrate and 50 μg of protein from the mouse liver 16K fraction.

RESULTS AND DISCUSSION

Mouse Liver 16K Fraction. We tested the 16K (light mitochondria) fraction of mouse liver, which contains peroxisomes, for its ability to metabolize *all-trans*-retinol and *all-trans*-retinal. The 16K fraction catalyzed conversion of *all-trans*-retinol into *all-trans*-retinal in a protein-dependent manner, but to the same extent after incubation for 5 min at 25 °C, for 5 min at 37 °C, or for 0 min at 4 °C (Figure 1A). To confirm the lack of temperature and time effects on retinol dehydrogenation, the reaction was repeated for 0 and 10 min at 25 and 37 °C (Figure 1C). Similar amounts of product were generated in the zero time control and during incubation for 10 min at both temperatures. These data are not consistent with enzymatic dehydrogenation of retinol by the mouse liver 16K fraction. In contrast, reduction of *all-trans*-retinal by the mouse liver 16K fraction was protein-, time-, and temperature-dependent, consistent with an enzymatic reaction (Figure 1B,C).

Effect of Clofibrate on Retinal Reductase Activity in the Liver 16K Fraction. Mice were treated with the peroxisome proliferator clofibrate to determine whether changes in the number of peroxisomes or induction of peroxisome enzymes affects retinal reduction. After 14 days, the 16K fractions of the clofibrate-dosed groups from two independent experiments showed an average ~2-fold increase in protein, an average ~2-fold increase in specific activity of retinal

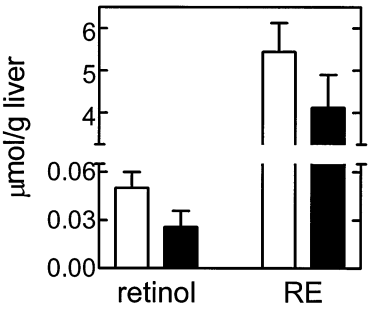

FIGURE 2: Retinol and retinyl ester concentrations (micromoles per gram of liver) in mice treated with clofibrate. Measurements were taken on the livers of mice from experiment 2 of Table 1. Data are the means ± standard error of the mean of five animals in each group (vehicle only, white bars; clofibrate dosed, black bars). The retinol concentrations were significantly different from each other ($p < 0.05$).

reduction, and an average 4-fold increase in retinal reductase units (Table 1). The increase in protein is consistent with clofibrate-induced peroxisome proliferation. Increases in both the specific activity and the number of reductase units, with a greater increase in the number of units, indicate that clofibrate induced specific expression of retinal-reducing enzymes(s), in addition to increasing total reductase(s) content through peroxisome proliferation. The 16K fractions from experiment 2 were assayed for the peroxisome protein catalase. Consistent with previous reports, clofibrate affected catalase activity and content, verifying proliferation of peroxisomes in the 16K fraction (*27*).

The retinol and retinyl ester content differed in livers between the two groups of mice in experiment 2 of Table 1. Clofibrate-treated mice had only ~50% of the liver retinol of control mice, demonstrating that clofibrate treatment decreases the concentration of hepatic retinol *in vivo* (Figure 2).

Reductase cDNA. A human peroxisomal SDR, which has not been tested with, retinoids, has been reported as a 2,4-dienoyl-CoA reductase (*31*). The NCBI database includes the mouse homologue of the "2,4-dienoyl-CoA" reductase as a putative retinal reductase activity (*32*). We amplified an 840-nucleotide cDNA of the peroxisomal 2,4-dienoyl-CoA reductase starting from mouse liver RNA. The cDNA contained three possible initiator sites. Use of the first initiator methionine would encode a protein with a deduced primary structure of 279 amino acid residues (Figure 3). The mouse SDR was identical with its human ortholog in all functional motifs, including the cofactor binding, catalytic, and peroxisome signaling residues and the "LVSNAA" fold, and the overall amino acid sequence of the mouse SDR was 80% identical with that of its human ortholog (Table 2).

The SDR, named RRD for retinal reductase, lacked a hydrophobic signal sequence like the one in the microsomal enzyme mRDH1. Instead, the first 28 N-terminal amino acid residues contained five positively charged residues and five residues with hydroxyl groups. The cofactor binding site at ^{39}TA(X)$_3$XG had a conservative substitution, instead of the typical TG(X)$_3$GXG sequence. The prototypical SDR residues LVNNAG were substituted in RRD with ^{124}LVSNAA (*33*). These differences may reflect the enhanced reactivity with NADPH versus NADH (see below), because the latter sequence also participates in cofactor binding. Catalytic residues were in the same locus as other SDRs, namely, ^{170}S-

```
          1                                                  50
mouse     MQKAGRLLGGWTQAWMSVRMASSGLTRRNPLSNKVALVTASTDGIGFAIA
human     MHKAG-LLGLCARAWNSVRMASSGMTRRDPLANKVALVTASTDGIGFAIA
          51                                                 100
mouse     RRLAEDGAHVVVSSRKQQNVDRAVATLQGEGLSVTGIVCHVGKAEDREKL
human     RRLAQDGAHVVVSSRKQQNVDQAVATLQGEGLSVTGTVCHVGKAEDRERL
          101                                                150
mouse     ITTALKRHQGIDILVSNAAVNPFFGNLMDVTEEVWDKVLSINVTATAMMI
human     VATAVKLHGGIDILVSNAAVNPFFGSIMDVTEEVWDKTLDINVKAPALMT
          151                                                200
mouse     KAVVPEMEKRGGGSVVIVGSVAGFTRFPSLGPYNVSKTALLGLTKNFAAE
human     KAVVPEMEKRGGGSVVIVSSIAAFSPSPGFSPYNVSKTALLGLTKTLAIE
          201                                                250
mouse     LAPKNIRVNCLAPGLIKTRFSSVLWEEKAREDFIKEAMQIRRLGKPEDCA
human     LAPRNIRVNCLAPGLIKTSFSSMLWMDKEKEESMKETLRIRRLGEPEDCA
          251                  279
mouse     GIVSFLCSEDASYINGETVVVGGGTPSRL
human     GIVSFLCSEDASYITGETVVVGGGTPSRL
```

FIGURE 3: Deduced amino acid sequence of mouse and human RRD. Boldface denotes cofactor binding, catalytic, and peroxisome targeting residues; underlining denotes residues that differ between mouse and human RRD. The box indicates the residues used to raise the anti-peptide antibody.

(X)$_{12}$Y(X)$_3$K. The last three residues of RRD, SRL, function as a type 1 peroxisome targeting signal (*34*, *35*). Other than these features, the mouse RRD does not have a sequence that is highly similar with that of any other known SDR.

Activity of Recombinant RRD in Intact Cells. mRRD and mRDH1 were expressed in CHO cells to evaluate and compare their activities with retinoids. In intact cells, RDH1 catalyzed dehydrogenation of *all-trans*-retinol into *all-trans*-retinal, as reported previously (*15*). RRD-transfected cells, in contrast, were no different from mock-transfected cells in generating *all-trans*-retinal from *all-trans*-retinol (Figure 4A). Mock-transfected CHO cells reduced *all-trans*-retinal, indicating that the cells harbor reductases, but transfection with the RRD cDNA increased the level of retinal reduction by 50% relative to that with the mock-transfected cells, and provided a net 60 pmol of retinol per plate of cells per assay. mRDH1, in contrast, did not support retinal reduction; it decreased the net amount of retinol by ~20% relative to that for the mock-transfected cells, suggesting that mRDH1 used as a substrate the retinol generated from retinal by the endogenous CHO cell reductase(s). These data indicate that mRRD and mRDH1 function as a reductase and a dehydrogenase, respectively, in intact cells.

Activity of Recombinant RRD in Cell Lysates. RRD, in the 880*g* supernatant of transfected CHO cells, catalyzed *all-trans*-retinal reduction in the presence of NADPH, but did not support *all-trans*-retinol dehydrogenation in the presence of NADP$^+$, consistent with the activity in intact cells (Figure 4B). NADPH was at least 30-fold more effective than NADH in supporting reduction by RRD. RRD reduced 13-*cis*-retinal and 9-*cis*-retinal at 28 and <2% to the extent observed with *all-trans*-retinal, respectively. These data obtained with intact CHO cells and CHO cell lysates indicate that RRD functions as an NADPH-dependent *all-trans*-retinal reductase, and are consistent with the observations made with the mouse 16K fraction.

Kinetic constants of RRD with *all-trans*-retinal were determined under initial velocity conditions. Recombinant RRD reduced free retinal (not bound with CRBP) with a $K_{0.5}$ value of 2.3 μM and a Hill constant of 1.7, and reduced CRBP(I)-bound retinal [2-fold molar excess of CRBP(I) at each retinal concentration] with a $K_{0.5}$ value of 8.6 μM and a Hill constant of 2.1 (means of two or three determinations) (Figure 5A). Reduction of 25 μM retinal in the absence of

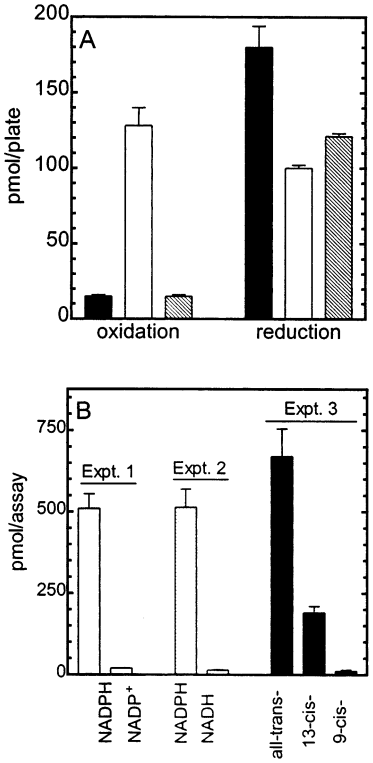

FIGURE 4: Reaction characteristics of recombinant RRD. (A) Oxidation of *all-trans*-retinol or reduction of *all-trans*-retinal was assessed in intact CHO cells transfected with pcDNA3/RDH1 (white bars) or pcDNA3/RRD (black bars) or mock-transfected cells (cross-hatched bars). Substrates (2 μM) were incubated for 30 min. Data are in units of picomoles of product per plate of CHO cells per assay (means $\pm$ standard deviation, $n = 3$). (B) RRD reactivity was measured in three separate experiments in the 800*g* lysates of pcDNA3/RRD-transfected cells. The first compared the rates of *all-trans*-retinal reduction supported by NADPH and *all-trans*-retinol dehydrogenation supported by $NADP^+$. The second compared *all-trans*-retinal reduction supported by NADPH or NADH. The third compared NADPH-supported reduction of *all-trans*-retinal, 13-*cis*-retinal, and 9-*cis*-retinal. Substrate concentrations were 5 μM; cofactor concentrations were 2 mM, and 5 μg of protein was used per assay. Data are in units of picomoles of product per assay (means $\pm$ standard deviation, $n = 3$). The 800*g* supernatant of mock-transfected cells generated less than 10 pmol of retinal/assay and <5 pmol of retinol/assay.

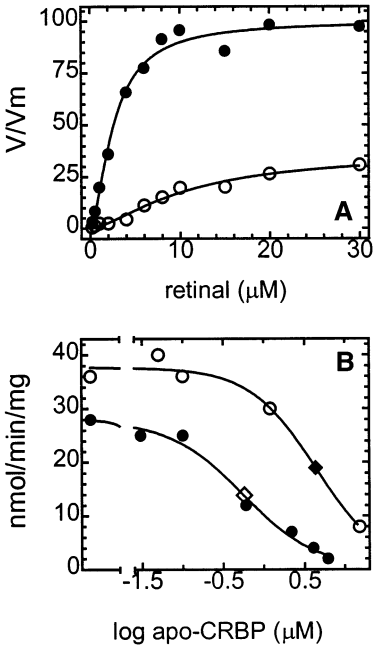

FIGURE 5: Kinetics of recombinant mouse RRD. (A) The 800*g* supernatant of a lysate of CHO cells transfected with pcDNA3/RRD was analyzed for reduction of "free" retinal (●) or retinal in the presence of a 2-fold molar excess of CRBP(I) (○). Rates were normalized to the V_m value of the reaction with free retinal. (B) The effects of graded concentrations of CRBP(I) were tested on the rates of RRD reduction of 4 (●) or 15 μM retinal (○). The *X*-axis shows the log apo-CRBP(I) concentration. Diamonds indicate the IC_{50} values for apo-CRBP(I). Data in both panels were fit with the nonlinear regression program GraphFit 4.

CRBP(I), or in the presence of 50 μM CRBP(I), under initial velocity conditions gave V_m values of 40 $\pm$ 1 and 14 $\pm$ 1 nmol min^{-1} (mg of protein)$^{-1}$, respectively (means $\pm$ standard deviation, $n = 4$). Both the $K_{0.5}$ values and the Hill constants were greater for RRD-catalyzed *all-trans*-retinal reduction in the presence of CRBP(I) than with "free" retinal. This shows that apo-CRBP(I) has a substrate [CRBP(I)-retinal] concentration-related impact on the rate of retinal reduction.

To confirm the observation of RRD inhibition by apo-CRBP(I), rates of reduction were determined from 4 and 15 μM retinal in the presence of graded CRBP(I) concentrations. The log apo-CRBP(I) concentration at each concentration of total CRBP(I), calculated with a K_d of 0.1 μM (*36*), was plotted against the rate of retinal reduction (Figure 5B). Rates of reduction were not decreased when the total CRBP(I) concentrations were lower than the retinal concentrations. Because adding CRBP(I) would lower the concentrations of free retinal to produce CRBP(I)-retinal, these data further show (along with the substrate−velocity data) that RRD must access both free and CRBP(I)-bound retinal. Adding total CRBP(I) concentrations equal to or greater than the retinal concentration decreased reduction rates substantially, but the rate with the lower retinal concentration was affected to a greater extent than the rate with the higher retinal concentration: the IC_{50} of apo-CRBP(I) was 0.6 μM with 4 μM retinal and 4.4 μM with 15 μM retinal. These data show that CRBP(I)-retinal serves as a substrate for RRD as efficiently as free retinal, but apo-CRBP(I) inhibits the reaction. The greater effect of apo-CRBP(I) at lower CRBP(I)-retinal concentrations is consistent with competition between apo- and holo-CRBP(I) for RRD.

mRNA Expression of RRD. RRD mRNA was expressed most intensely in liver, kidney, heart, and testis by Northern blot analysis, with much less intense but detectable expression in brain, spleen, and lung (Figure 6). Dot-blot analysis confirmed mRNA expression in these tissues and revealed expression in most tissues that were assayed. Submaxillary gland and epididymus had the most intense expression of the tissues not assayed by Northern blotting. Notably, the dot blot extended expression insight to most gonadal tissues and to embryonic days 7, 11, 15, and 17. None of the controls exhibited signals.

Effect of Clofibrate on the RRD Protein in the Mouse Liver 16K Fraction. To determine whether the amount of RRD protein increased with the increase in the level of retinal reduction in the 16K fraction from clofibrate-treated mice, Western blots were performed on the liver samples from experiment 2 of Table 1. The 5-fold increase in reductase units, noted in the clofibrate-treated group of experiment 2, was accompanied by an ~5-fold increase in the total amount

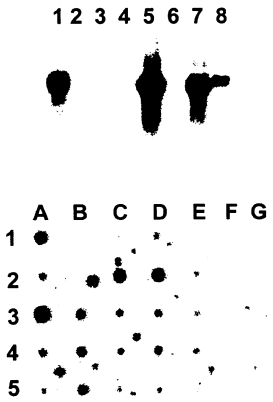

FIGURE 6: Tissue expression of RRD mRNA. In the top panel, Northern blot hybridization was carried out with poly(A^+) mRNA from (1) heart, (2) brain, (3) spleen, (4) lung, (5) liver, (6) skeletal muscle, (7) kidney, and (8) testis. In the bottom panel, dot-blot hybridization was carried out with poly(A^+) mRNA from (A1) kidney, (A2) lung, (A3) liver, (A4) eye, (A5) brain, (B1) empty, (B2) empty, (B3) smooth muscle, (B4) skeletal muscle, (B5) heart, (C1) spleen, (C2) submaxillary gland, (C3) thymus, (C4) thyroid, (C5) pancreas, (D1) uterus, (D2) epididymus, (D3) prostate, (D4) ovary, (D5) testis, (E1) empty, (E2) embryo on day 17, (E3) embryo on day 15, (E4) embryo on day 11, (E5) embryo on day 7, (F1) empty, (F2) *Escherichia coil* DNA, (F3) *E. coli* rRNA, (F4) yeast tRNA, (F5) yeast total RNA, (G1) empty, (G2) mouse DNA, (G3) mouse DNA, (G4) Cot 1 DNA, and (G5) poly[r(A)].

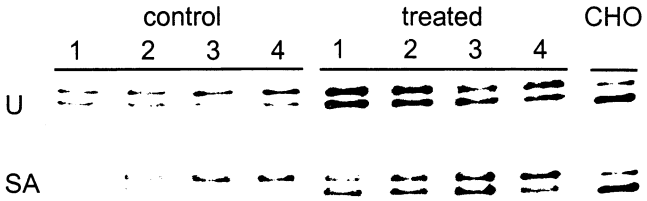

FIGURE 7: Western blot analyses of the mouse liver 16K fraction. Protein samples from the 16K fractions of liver from mice in experiment 2 were analyzed by the Western blot method with anti-RRD peptide antibody. The lane labeled CHO shows Western blotting of RRD expressed in transfected CHO cells (5 μg of the 800*g* lysate protein). The lower signal represents the majority of RRD. The U row shows the total amount of RRD expressed; each sample represents the same percentage of total peroxisome protein (micrograms): C1, 15; C2, 20; C3, 20; C4, 19; T1, 33; T2, 35; T3, 30; and T4, 33. The SA row shows RRD expression in 20 μg of 16K protein from each mouse. Band densities were quantified with the Molecular Analyst program. The mean $\pm$ standard deviation for the U row lower control signals was 34 $\pm$ 13 (arbitrary units) and for the U row lower treated signals was 180 $\pm$ 70. Densities on the signals from the control mice in the SA row could not be obtained reliably because of their low intensities.

of RRD protein (Figure 7). Comparison of equivalent amounts of the 16K fraction protein also showed an RRD increase in the treated mice, reflecting the increase in specific reductase activity. The reason for the two bands in the Western blots is unknown. Perhaps RRD undergoes post-translational modifications, or is translated at different start sites. Observation of two bands in the CHO cell lysate is consistent with either of these suggestions.

Concluding Summary. Human 2,4-dienoyl-CoA reductase was identified and cloned by immunoaffinity selection with antibodies raised against peroxisome proteins, and was further experimentally verified as a peroxisome protein by double immunofluorescence in intact cells (*31*). The mouse homologue of human 2,4-dienoyl-CoA reductase has the identical peroxisome targeting sequence, PTS-1, and identical

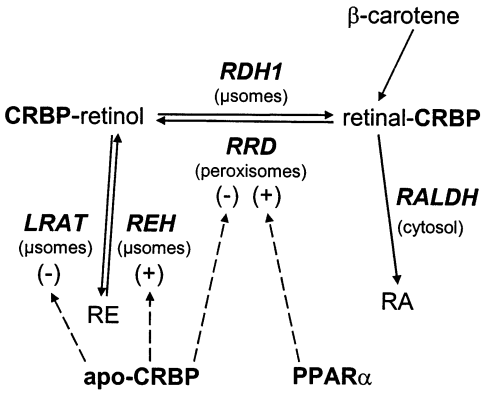

FIGURE 8: Model proposed for the contribution of RRD to retinoid homeostasis. The data reported here are consistent with the hypothetical model in which RRD contributes to controlling retinol metabolism. Competition between RRD and retinal dehydrogenases (RALDH) for retinal could provide one mechanism for preventing excess atRA production. During adequate dietary β-carotene and vitamin A intake, most retinol would undergo esterification via LRAT to produce RE. During low or inadequate dietary β-carotene and vitamin A intake, mobilization of RE by retinyl ester hydrolase (REH) would provide retinol for atRA biosynthesis via RDHI and RALDH. Relatively high apo-CRBP(I) levels would occur during retinol inadequacy, inhibiting LRAT and accelerating RE hydrolysis. Relatively high apo-CRBP(I) levels also would inhibit RRD. Together, these actions would allow the continued flux of retinol into RA via RDH1 and RALDH. In contrast, PPARα agonists such as clofibrate accelerate retinol clearance, similar to their effects on the metabolism of other lipids.

cofactor binding and catalytic residues (*32*). Thus, the data reported previously (*31, 32*) and the current data connect mouse RRD (also known as human 2,4-dienoyl-CoA reductase) and retinal reduction in peroxisomes, and show that clofibrate, the peroxisome proliferator and PPARα agonist, catalyzes retinol turnover *in vivo*. PPARα, a type II nuclear receptor, regulates lipid metabolism by inducing peroxisome proliferation, fatty acid oxidation, ketone body synthesis, and adipocyte differentiation (*37, 38*). These data indicate that PPARα and peroxisomes are involved in retinoid metabolism. Notably, major organs of PPARα expression include liver, kidney, and heart, similar to the major sites of RRD expression (*39*).

A potential function of RRD could include reduction of retinal generated by carotenoid cleavage. Another possibility might include decreasing retinal concentrations as a fail-safe mechanism for containing RA biosynthesis. In this putative scenario, any retinal generated outside of a "specific" pathway, e.g., by cytochrome P450s or alcohol dehydrogenases, would be reduced to avoid ectopic RA biosynthesis. A third possibility might include competition of RRD with enzymes that generate RA *in vivo* to exert fine control over spatial−temporal RA biosynthesis.

The mechanism(s) whereby RRD-catalyzed retinal reduction might promote retinol turnover is not clear. Oxidative metabolism of retinol, however, might occur in concert with retinal generated by RRD and other reductases, causing a decrease in retinol concentrations.

Interestingly, CRBP(I), the physiological carrier of intracellular retinol ($K_d \sim 0.1$ nM) and a potential carrier of retinal ($K_d \sim 100$ nM) (*36*), affects the efficiency of RRD, most likely through competition between apo-CRBP(I) and holo-CRBP(I). This is reminiscent of the effects exerted by the apo-CRBP(I)/CRBP(I)-retinol ratio on the relative rates of

RE hydrolysis versus RE synthesis. Lecithin:retinol acyltransferase (LRAT) recognizes CRBP(l)-retinol as substrate for producing retinyl esters, and is inhibited by apo-CRBP-(I). This provides a mechanism for connecting the rate of RE formation to retinol availability (*40*). In addition, apo-CRBP(I) stimulates the rate of hydrolysis of endogenous microsomal RE (*41*, *42*). These actions would channel retinol from RE formation to RE mobilization during retinol insufficiency, presumably to provide substrate for RA biosynthesis. The arrest of RRD-catalyzed retinal reduction by apo-CRBP(I), especially at lower retinal concentrations, seems complementary to the effects of apo-CRBP(I) on retinol esterification and mobilization; namely, apo-CRBP(I) may serve as a signal of low retinoid availability that directs the flux of retinoid metabolism away from storage and/or catabolism and toward the biosynthesis of RA (Figure 8).

REFERENCES

1. Lotan, R. (1988) *Prog. Clin. Biol. Res. 259*, 261−271.
2. Wolf, G. (1984) *Physiol. Rev. 64*, 674−937.
3. Staels, B. (2001) *J. Am. Acad. Dermatol. 45*, S158−S167.
4. Stephensen, C. B. (2001) *Annu. Rev. Nutr. 21*, 167−192.
5. Maden, M. (2000) *Proc. Nutr. Soc. 59*, 65−73.
6. Dawson, M. I. (2000) *Curr. Pharm. Des. 6*, 311−325.
7. Harrison, E. H., and Hussain, M. M. (2001) *J. Nutr. 131*, 1405−1408.
8. von Lintig, J., and Wyss, A. (2001) *Arch. Biochem. Biophys. 385*, 47−52.
9. Redmond, T. M., Gentleman, S., Duncan, T., Yu, S., Wiggert, B., Gantt, E., and Cunningham, F. X., Jr. (2001) *J. Biol. Chem. 276*, 6560−6565.
10. Napoli, J. L. (2000) *Nutr. Rev. 58*, 230−236.
11. Nagpal, S., and Chandraratna, R. A. (1998) *Curr. Opin. Clin. Nutr. Metab. Care 1*, 341−346.
12. McEwan, l. J. (2000) *Biochem. Soc. Trans. 28*, 369−373.
13. Mark, M., Ghyselinck, N. B., Wendling, O., Dupe, V., Mascrez, B., Kastner, P., and Chambon, P. (1999) *Proc. Nutr. Soc. 58*, 609−613.
14. Napoli, J. L. (1999) *Biochim. Biophys. Acta 1440*, 139−162.
15. Zhang, M., Chen, W., Smith, S. M., and Napoli, J. L. (2001) *J. Biol. Chem. 276*, 44083−44090.
16. Newcomer, M. E. (1995) *FASEB J. 9*, 229−239.
17. Noy, N. (2000) *Biochem. J. 348*, 481−495.
18. Luu, L., Ramshaw, H., Tahayato, A., Stuart, A., Jones, G., White, J., and Petkovich, M. (2001) *Adv. Enzymol. Regul. 41*, 159−175.
19. Stocco, D. M. (2001) *Annu. Rev. Physiol. 63*, 193−213.
20. Ruff, S. J., and Ong, D. E. (2000) *FEBS Lett. 487*, 282−286.
21. Wanders, R. J. (2000) *Cell Biochem. Biophys. 32*, 89−106.
22. Nagao, A., and Olson, J. A. (1994) *FASEB J. 8*, 968−973.
23. Kakkad, B. P., and Ong, D. E. (1988) *J. Biol. Chem. 263*, 12916−12919.
24. deDuve, C., Pressman, B. C., Gianetto, R., Wattiaux, R., and Appelmans, F. (1955) *Biochem. J. 59*, 433−438.
25. Leighton, F., Poole, B., Beaufay, H., Baudhin, P., Coffer, J., Fowler, W., and deDuve, C. (1969) *J. Cell Biol. 37*, 482−513.
26. Ghosh, M. K., and Hajra, A. K. (1986) *Anal. Biochem. 159*, 169−174.
27. Aebi, H. (1984) *Methods Enzymol. 105*, 121−126.
28. Bradford, M. M. (1976) *Anal. Biochem. 72*, 248−254.
29. Schmidt, C. K., Volland, J., Hamscher, G., and Nau, H. (2002) *Biochim. Biophys. Acta 1583*, 237−251.
30. Chai, X., Zhai, Y., and Napoli, J. L. (1997) *J. Biol. Chem. 272*, 33125−33131.
31. Fransen, M., Van Veldhoven, P. P., and Subramani, S. (1999) *Biochem. J. 340*, 561−568.
32. Furukawa, A., Huang, D., Ohnishi, T., and Ichikawa, Y. (2000) NCBI entries AB045131 and AB045132.
33. Bailey, T. L., Baker, M. E., and Elkan, C. P. (1997) *J. Steroid Biochem. Mol. Biol. 2*, 29−44.
34. Subramani, S., Koller, A., and Synder, B. W. (2000) *Annu. Rev. Biochem. 69*, 399−448.
35. Hettema, E. H., Distel, B., and Tabak, H. F. (1999) *Biochim. Biophys. Acta 1451*, 17−34.
36. Li, E., Qian, S. J., Winter, N. S., d'Avignon, A., Levin, M. S., and Gordon, J. I. (1991) *J. Biol. Chem. 266*, 3622−3629.
37. Schoonjans, K., Martin, G., Staels, B., and Auwerx, J. (1997) *Curr. Opin. Lipidol. 5*, 274−289.
38. Desvegne, B., and Wahli, W. (1999) *Endocr. Rev. 20*, 649−688.
39. Issemann, I., and Green, S. (1990) *Nature 347*, 645−650.
40. Herr, F., and Ong, D. E. (1992) *Biochemistry 31*, 6748−6755.
41. Ottonello, S., Petrucco, S., and Mariani, G. (1987) *J. Biol. Chem. 262*, 3975−3939.
42. Boerman, M. H. E. M., and Napoli, J. L. (1991) *J. Biol. Chem. 266*, 22273−22278.

BI026948I